The EMBO Journal (2013), 1–12
www.embojournal.org

OPEN ACCESS TRANSPARENT PROCESS

THE EMBO JOURNAL

Regulation of cerebral cortex size and folding by expansion of basal progenitors

Miki Nonaka-Kinoshita[1], Isabel Reillo[2], Benedetta Artegiani[1], Maria Ángeles Martínez-Martínez[2], Mark Nelson[3], Víctor Borrell[2,*] and Federico Calegari[1,*]

[1]CRTD-DFG Research Centre for Regenerative Therapies Dresden, Technische Universität Dresden, Dresden, Germany, [2]Instituto de Neurociencias, CSIC & Universidad Miguel Hernández, San Juan de Alicante, Spain and [3]Echelon Biosciences 675, Salt Lake City, UT, USA

Size and folding of the cerebral cortex increased massively during mammalian evolution leading to the current diversity of brain morphologies. Various subtypes of neural stem and progenitor cells have been proposed to contribute differently in regulating thickness or folding of the cerebral cortex during development, but their specific roles have not been demonstrated. We report that the controlled expansion of unipotent basal progenitors in mouse embryos led to megalencephaly, with increased surface area of the cerebral cortex, but not to cortical folding. In contrast, expansion of multipotent basal progenitors in the naturally gyrencephalic ferret was sufficient to drive the formation of additional folds and fissures. In both models, changes occurred while preserving a structurally normal, six-layered cortex. Our results are the first experimental demonstration of specific and distinct roles for basal progenitor subtypes in regulating cerebral cortex size and folding during development underlying the superior intellectual capability acquired by higher mammals during evolution.

The EMBO Journal advance online publication, 26 April 2013; doi:10.1038/emboj.2013.96
Subject Categories: development; neuroscience
Keywords: basal progenitors; brain evolution; mammalian neural stem cells; mouse brain development; neurogenesis

Introduction

The size and shape (topology) of the mammalian cerebral cortex present significant variations across species, ranging from the small and smooth (lissencephalic) cortex of mice, to the large and profoundly folded (gyrencephalic) cortex of humans. Cortical topology is determined during embryonic development and reflects the balance between radial and tangential growth of the neuronal layers. According to the radial unit hypothesis (Rakic, 1995), radial size (thickness) is determined by the number of neurons generated per radial unit, or column, of cortex while tangential size (surface area) depends on the number of such radial units.

Radial units are established by radial glia cells (RGCs) that are located in the ventricular zone (VZ) and that for long were thought to be only a scaffold supporting the radial migration of newborn neurons (Rakic, 1995). Later, it was found that RGCs are neural stem cells (Malatesta *et al*, 2000; Miyata *et al*, 2001; Noctor *et al*, 2001; Gotz and Huttner, 2005) serving also as a source of unipotent neurogenic basal progenitors (BPs), which delaminate from the VZ to form the subventricular zone (SVZ) and become the primary source of cortical neurons (Haubensak *et al*, 2004; Miyata *et al*, 2004; Noctor *et al*, 2004; Gotz and Huttner, 2005). Upon the discovery of BPs, it was proposed that their abundance relative to RGCs determines both size and folding of the cerebral cortex (Kriegstein *et al*, 2006; Molnar *et al*, 2006). However, soon after the formulation of this hypothesis, it was found that RGCs also generate a second subtype of basal progenitor referred to as basal radial glia (bRG) which, while also delaminating from the VZ, retains properties similar to RGCs including pial contact and multipotency (Fietz *et al*, 2010; Hansen *et al*, 2010; Reillo *et al*, 2011). bRG cells are abundant in gyrencephalic brains but very scarce in lissencephalic rodents (Shitamukai *et al*, 2011; Wang *et al*, 2011; Reillo and Borrell, 2012) and their retention of a pial, but not apical, process is thought to introduce curvature in the developing cerebral cortex (Fietz and Huttner, 2011; Lui *et al*, 2011; Borrell and Reillo, 2012). Hence, the latest hypotheses propose that cortical size and folding may depend not only on the relative abundance of RGCs and BPs but also on the balanced proliferation of bRG cells (Fietz and Huttner, 2011; Lui *et al*, 2011; Borrell and Reillo, 2012).

Multiple lines of evidence either supporting or challenging these hypotheses have been alternatively reported, which evidences the difficulties emerging while studying mechanisms of brain development across evolution. One of the major difficulties has been to manipulate the proliferation of specific progenitor subtypes while preserving a correct cortical lamination and structure. Specifically, several transgenic mouse lines have been generated in which the balance between RGC and BP proliferation was profoundly altered. Although cortical topology in these mice was severely perturbed, none succeeded in developing a coherent six-layered cortex (Chenn and Walsh, 2002; Cappello *et al*, 2006; Siegenthaler *et al*, 2009). In contrast, electroporation of Cdk4 and cyclin D1 (4D) successfully promoted BP expansion without altering cortical lamination (Lange *et al*, 2009), but no change in cortical topology could be observed because electroporation only affected a small proportion of progenitor cells. Finally, addressing the role of bRG cells in cortical topology requires the use of gyrencephalic

*Corresponding authors. V Borrell, Instituto de Neurociencias, CSIC & Universidad Miguel Hernández, Av. Ramón y Cajal s/n, San Juan de Alicante, Spain. Tel.: +34 96 591 9245; Fax: +34 96 591 9561; E-mail: vborrell@umh.es or F Calegari, CRTD-DFG Research Centre for Regenerative Therapies Dresden, Technische Universität Dresden, Dresden, Germany. Tel.: +49 35 14 588 2204; Fax: +49 35 14 588 2209; E-mail: federico.calegari@crt-dresden.de

Received: 4 March 2013; accepted: 5 April 2013

species because the abundance of this cell type in rodents is negligible (Shitamukai *et al*, 2011; Wang *et al*, 2011; Reillo and Borrell, 2012), yet no manipulation of progenitor subtypes has been performed in gyrencephalic species *in vivo* to date.

To overcome these limitations we generated a transgenic mouse line that allows us to control BP cell proliferation in a tissue-specific, temporal and reversible manner during embryonic brain development by means of 4D overexpression. In addition, we used 4D overexpression in the naturally gyrencephalic ferret to further expand bRG cells *in vivo* and thus investigate the role of this progenitor subtype in the establishment of cortical size and folding. Remarkably, while increases in progenitor cell proliferation led to larger cortical surface area in both experimental models, cortical folding was induced exclusively in the already gyrencephalic ferret but not in the lissencephalic mouse, challenging previous hypotheses (Rakic, 1995; Kriegstein *et al*, 2006; Molnar *et al*, 2006). Our findings are the first experimental demonstration that distinct subtypes of basal progenitor cells play different roles in defining cerebral cortex topology during development.

Results

Generation of the nestin^{rtTA}/tetbi^{4D} mouse line

In order to expand the number of BP cells in the developing mouse cerebral cortex, we began by generating a transgenic line where 4D could be overexpressed in cortical progenitors with reliable temporal control. To this aim we designed a bidirectional tetracycline-dependent transactivator minimal Tet promoter (*tetbi*) driving the expression, on opposite directions, of Cdk4 and cyclin D1, each linked to luciferase or red fluorescent protein (RFP), respectively, by self-cleaving 2A peptides (de Felipe *et al*, 2006) (Figure 1A, top). Luciferase assays and western blot analyses in rtTA-expressing HEK-293 cells revealed that the *tetbi*^{4D} construct was effective in triggering doxycycline-dependent expression of catalytically active 4D together with luciferase and RFP under the same *tetbi* promoter, and that overexpressed 4D triggered hyperphosphorylation of retinoblastoma *in vitro* (Figure 1B). Several *tetbi*^{4D} responder lines were then generated by pronuclear injection. Expression of the 4D cassette in presence of doxycycline, and leakiness in its absence, was tested using primary cultures of *tetbi*^{4D} embryonic fibroblasts as a proxy for transgene induction after transfection with rtTA plasmids followed by RFP/luciferase assays (Figure 1C). The founder line, whose fibroblasts revealed the strongest level of induction and minimal leakiness, was finally crossed with the previously described *nestin*^{rtTA} line (Mitsuhashi *et al*, 2001) (Figure 1A, bottom) to generate the bigenic *nestin*$^{rtTA+/+}$/*tetbi*$^{4D+/-}$ line, referred to as 4D line for simplicity. Various protocols of tetracycline administration in 4D mouse embryos were investigated including different routes of delivery, frequency and concentration of either doxycycline or its analogue 9-tert-butyl doxycycline (9TB-dox), which has been reported to trigger higher induction due to its increased binding affinity and permeability through lipids (Zhu *et al*, 2007). Indeed, 9TB-dox was about 10-fold more potent than normal doxycycline as judged by RFP expression, with two

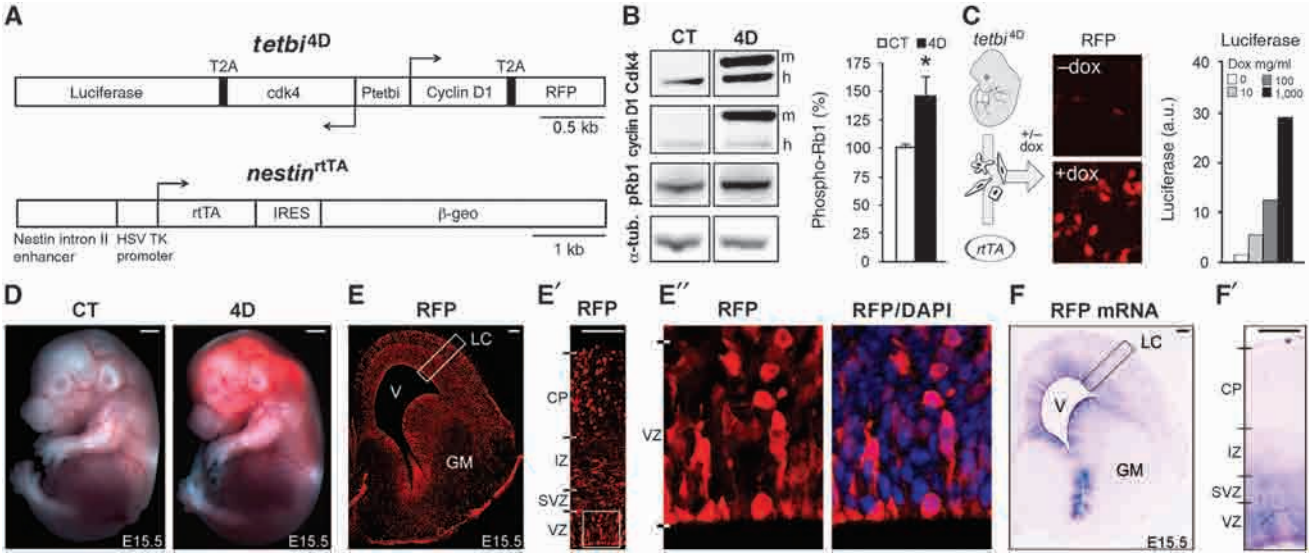

Figure 1 Generation of 4D mice. (**A**) Drawings representing the constructs used to generate the transactivator (*nestin*^{rtTA}) and responder (*tetbi*^{4D}) line. Note the use of 2 A peptide to trigger the stoichiometric expression of Cdk4 and cyclin D1 together with the reporter genes. (**B**) Western blot analyses (left) and quantification of retinoblastoma phosphorylation (pRb1) (right) in HEK-293 cells transfected with RFP (CT) or *tetbi*^{4D} (4D) constructs together with rtTA expression vectors followed by doxycycline treatment. Note the appearance of mouse (m), in addition to human (h), Cdk4 and cyclin D1 with higher molecular weight due to the presence of 2 A peptides as well as the increased pRb1 phosphorylation in 4D. (**C**) Approach used to identify the best responder, 4D founder line by luciferase assays in primary embryonic fibroblasts transfected with rtTA expression vectors followed by administration of doxycycline. Note the doxycycline-specific appearance of RFP (middle) and the dose-dependent expression of luciferase with minimal leakiness (right). (**D**) Whole mount, fluorescence pictures of E15.5 littermate embryos showing endogenous RFP fluorescence in 4D (right) but not CT (left) after 9TB-dox administration starting at E11.5. (**E** and **E″**) Fluorescence pictures of a coronal hemisphere section (**E**) and magnified views (white boxes in **E** and **E′** shown in **E′** and **E″**, respectively) of a 4D embryo treated as in (**D**) after immunohistochemistry for RFP and DAPI counterstain (blue). (**F** and **F′**) Bright field pictures of a coronal section as in (**E**) after *in situ* hybridisation for RFP mRNA. Data are mean ± s.e.m.; $^*P<0.05$; $n=3$. GM, ganglionic eminence; LC, lateral cortex; V, ventricle. Scale bars = 500 μm (**D**) or 100 μm (**E**–**F′**).

daily intraperitoneal injections of 1 mg achieving the maximal effect (data not shown).

To obtain a similar proportion of control (CT) (*nestin*$^{rtTA+/+}$/*tetbi*$^{4D-/-}$) and 4D (*nestin*$^{rtTA+/+}$/tetbi$^{4D+/-}$) embryos within the same litter we crossed *nestin*$^{rtTA+/+}$ with bigenic *nestin*$^{rtTA+/+}$/*tetbi*$^{4D+/-}$ mice. Pregnant females received 9TB-dox injections starting at embryonic day (E) 11.5 (onset of cortical neurogenesis) and embryos were subsequently analysed at different developmental times. Under these conditions, endogenous RFP fluorescence could be detected as soon as 24 h after the first administration of 9TB-dox. Intensity levels of RFP at 24 h were undistinguishable from those after 4 days of continuous treatment (Figures 1D and E and data not shown), suggesting that maximal transgene expression was already reached within the first day. RFP fluorescence was detected along the entire central nervous system of 4D embryos (Figure 1D; right), while no expression was observed neither in CT embryos (Figure 1D; left) nor in 4D mice without 9TB-dox treatment (data not shown).

RFP immunohistochemistry on brain sections revealed that 4D mice displayed mosaic RFP expression, with approximately 30–40% of cells in the VZ being RFP+ (Figures 1E–E″). This was unexpected because all RGCs are known to express nestin and, in fact, rtTA transcripts were detected throughout the entire VZ (Mitsuhashi *et al*, 2001) (data not shown). While this might suggest an underlying genetic bias towards a particular subpopulation of neural progenitors, we found that this was not the case because the same proportion to RFP+ cells was found within Tbr2− RGCs and Tbr2+ BPs (data not shown). While RFP mRNA was only detected within the VZ and SVZ (Figures 1F and F′), RFP+ cells were found throughout the other cortical layers as well (Figure 1E′) due to inheritance of RFP protein in migrating neurons. Finally, while 24 h of 9TB-dox administration were sufficient to trigger detectable RFP expression, no RFP transcripts could be observed by *in situ* hybridisation one day after a single injection of 9TB-dox (data not shown), indicating the fast activation/inactivation of the *tetbi*^{4D} cassette within 24 h after administration/withdrawal of 9TB-dox.

Altogether, these data show that the 4D line can be used to achieve acute, tissue-specific, on/off temporal control of catalytically active 4D expression in neural precursors during mammalian development. Importantly, despite the fact that our manipulation was effective only on a subpopulation of cells, we decided to assess the absolute numbers, rather than proportions, of different cell types in the whole brain because the mosaic expression of 4D, if any, would minimise the impact of our manipulation making a potential increase in tissue mass even more significant. Thus, cell types were assessed considering a fixed unit of cortical column (100 μm wide) at the level of field 40 of the lateral cortex (e.g., boxes in Figures 1E and F). Special care was given to comparing nearly identical rostral-to-caudal sections of 4D and CT littermate embryos identified by stereological analyses of the whole brain.

The use of nestin^{rtTA}/tetbi^{4D} mice allows the control of BP expansion and manipulation of brain morphogenesis

To test the potential of our strategy to expand cortical BPs, we began by forcing 4D expression in neural progenitors from E11.5 to E15.5 and analysing the effects at E15.5 (Figure 2A). The influence of 4D overexpression on the abundance of cycling progenitors was first assessed by a pulse of BrdU 5 h prior to fixation. We found that 4D embryos had an increased number of BrdU+ progenitors in the VZ (80%) and SVZ (31%) compared to CT littermate embryos, used throughout our study as internal negative controls (Figure 2B). To determine the identity of the supernumerary progenitor cells, we performed immunohistochemistry for Pax6 and Tbr2 as markers of RGCs and BPs, respectively (Englund *et al*, 2005). Tbr2+ cells were found significantly increased in the VZ and SVZ by 33% and 55%, respectively, whereas the abundance of Pax6+, as well as Pax6+/Tbr2−, RGCs was similar in both layers (Figure 2C and Supplementary Figures S1A–C). PH3 immunohistochemistry revealed that supernumerary Tbr2+ cells corresponded to BPs dividing in the SVZ, causing a 2.3-fold increase in mitotic cells in the SVZ of 4D embryos without change in the VZ (Figure 2D). Moreover, we observed a 1.9-fold increase in PH3+ cells in the intermediate zone (IZ)/cortical plate (CP) of 4D mice (although these were a very minor proportion of all cortical mitoses) (Figure 2D), suggesting that, in addition to BPs, 4D may trigger the expansion of the small population of bRGs found in mouse (Shitamukai *et al*, 2011; Wang *et al*, 2011). Assessment of Pax6+/Tbr2− cells in the IZ (hallmarks of bRG in mouse) revealed that bRGs were not expanded, as their abundance was similar in CT and 4D embryos (3.5 ± 1.1 and 3.6 ± 1.0 cells/100 μm, respectively; data not shown). In contrast, we found a 1.6-fold increase in Tbr2+/PH3+ cells in the IZ of 4D embryos, further confirming that the effect of 4D overexpression in the mouse brain is restricted to BPs (Figure 2D and data not shown).

Cortical development relies on a fine-tuned balance between the generation of progenitors and neurons. Thus, the increased generation of BPs in 4D embryos suggested that neurogenesis might in turn be reduced. To investigate effects on neurogenesis, we injected a pulse of BrdU at E12.5 and analysed the amount of postmitotic BrdU+ cells in the CP at E15.5. As predicted, 4D brains had 38% less BrdU+ cells than CT brains (Figure 2E). A similar decrease (27%) was also observed in the abundance of cells positive for Ctip2, a marker of early-born neurons (Figure 2F), thus confirming reduced neurogenesis in 4D brains. We also found that the SVZ in 4D embryos was 26% thicker than in CT embryos, while the CP was 18% thinner (Supplementary Figure S1C), substantiating our findings of a reciprocal amplification of BPs and reduction of neurogenesis (Figures 2B–F). In contrast, both thickness and surface area of the VZ remained unchanged (Figures 2B–F, Supplementary Figure S1C and data not shown). Taken together, our results show that 4D mice allowed us to systematically increase the abundance of BPs in the whole brain without affecting RGCs, resulting in topological changes of the developing cortex already at early stages of development.

A transient expansion of BPs increases cortical thickness of the embryonic brain

Our results are consistent with previous studies using electroporation which supported the notion that 4D influences BPs by specifically promoting their amplification at the expense of neurogenesis (Lange *et al*, 2009; Salomoni and Calegari, 2010). Beyond the local and acute effects of electroporation, 4D transgenic mice allowed us to expand BPs in the entire cortex and for extended periods of time, to

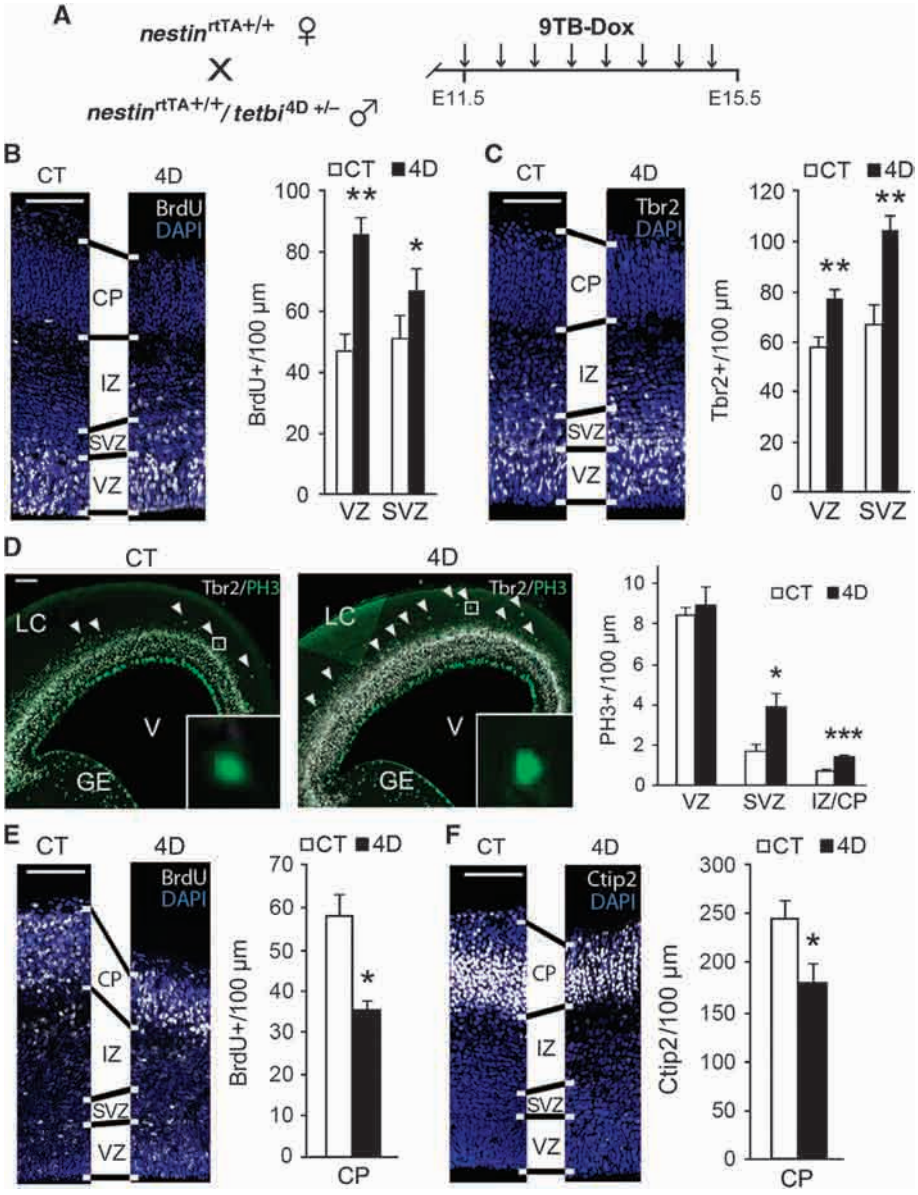

Figure 2 BPs expand at the expense of neurogenesis in 4D transgenic mouse embryos. (**A**) Experimental approach used to study the effect of 4D overexpression after continous administration of 9TB-Dox from E11.5 to E15.5, followed by sacrifice. (**B–F**) Fluorescence pictures and quantifications of cells labelled for various markers, as indicated in each panel, in cortices of E15.5 CT and 4D littermate embryos treated with 9TB-dox starting at E11.5. BrdU was administered either 5 h prior to sacrifice (**B**) or at E12.5 (**E**). Shown in each panel are coronal sections taken from an equivalent cortical region of CT and 4D littermates as identified by stereology. Note the change in thickness of cortical layers in each image pair (lines between panels). Scale bars, 100 µm. Data are mean ± s.e.m; $^{*}P<0.05$; $^{**}P<0.01$, $^{***}P<0.001$; $n>3$ pairs of embryos from different litters. See also Supplementary Figure S1.

thus investigate the potential consequences on brain development and topology of the cerebral cortex. Specifically, the power of the Tet-system is that it allows the transient on/off overexpression of transgenes. In this way, a phase of BP expansion can be followed by a switch back to their physiological differentiation, potentially resulting in an increased generation of neurons. Thus, we next investigated whether 9TB-dox withdrawal at E15.5 would allow the expanded pool of BPs to switch to neurogenesis, and then whether this would result in an increase in brain size at E18.5, the end of neurogenesis (Figure 3A). Following this protocol we found that at E18.5 a similar number of Tbr2+ cells were present in the VZ of CT and 4D embryos (Figure 3B), indicating that the generation of BPs from RGCs was restored to physiological levels. Regarding the SVZ, Tbr2+ cells did not continue to expand further but, similarly to E15.5, they remained 60% more numerous in 4D than in CT (Figure 3B). This suggested that after a transient expansion during 4D overexpression, BPs returned to a normal proportion of neurogenic vs. proliferative divisions. To investigate effects on neurogenesis, we analysed at E18.5 the abundance of cells in the CP labelled with BrdU at E15.5 (that is, late-born upper-layer neurons), as well as cells positive for the neuronal markers Satb2 and Ctip2. We found a 47% increase in BrdU+ cells in 4D compared to CT embryos, and a 23% and 32% increase in Satb2+ and

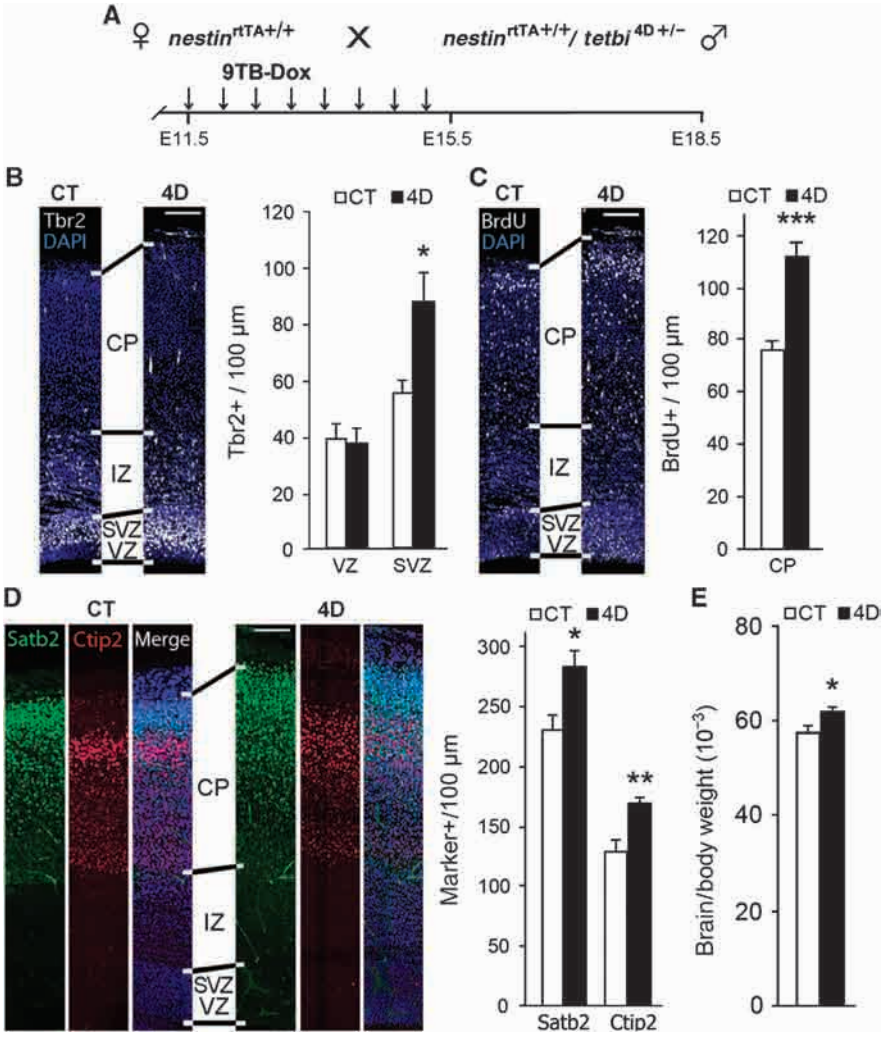

Figure 3 Increased cortical neuron production and encephalization after transient 4D overexpression. (**A**) Experimental approach used to study the effect of 4D overexpression after continous administration of 9TB-Dox from E11.5 to E15.5 followed by sacrifice at E18.5. (**B–D**) Fluorescence pictures and quantifications of cells labelled for various markers, as indicated in each panel, in E18.5 cortices of CT and 4D mice treated with 9TB-dox from E11.5 to E15.5 with BrdU (**C**) being administered at the end of 9TB-dox treatment. Shown are coronal sections from an equivalent cortical region of CT and 4D littermates. (**E**) Encephalization index calculated as brain weight relative to body mass. Scale bars, 100 µm. Data are mean ± s.e.m.; $*P<0.05$, $**P<0.01$, $***P<0.001$; $n=3$ (**B–D**) or 8 (**E**) pairs of embryos from at least three different litters. See also Supplementary Figure S2.

Ctip2+ cells, respectively (Figures 3C and D). Importantly, the laminar distribution and proportion of Satb2+ and Ctip2+ neurons were similar in CT and 4D embryos (Figure 3D) indicating that the observed changes were not due to altered cell migration, lamination or neuronal specification. Concomitant with a greater abundance of BPs and increased neurogenesis, 4D embryos displayed a thicker SVZ and CP (73% and 25% thicker, respectively), again without any significant change in ventricular or cortical surface area (Figures 3B–D and Supplementary Figure S2) but resulting in an 8% increase in encephalization (Figure 3E).

A transient expansion of BPs increases cortical surface area of the mature brain

The above observations seemed to indicate that expansion of BPs and increased neurogenesis result in increased cortical thickness rather than surface area, contradicting current hypotheses (Kriegstein *et al*, 2006; Borrell and Reillo, 2012). However, cortical development is not complete by E18.5 and significant topological differences could still emerge at later stages. To investigate this, we forced 4D expression from E11.5 to E15.5 as before, but now we analysed the brains at postnatal day (P) 21, when corticogenesis is complete (Figure 4A) (Molyneaux *et al*, 2007). At P21, 4D mice showed a 23% increase in encephalization compared to CT mice (Figure 4B), which was significantly greater than the difference observed at E18.5. However, contrary to E18.5, at P21 the thickness of the CP was virtually identical in 4D and CT mice, whereas cortical surface area was now 8% larger in 4D mice (Figure 4B; right).

Our data seemed in agreement with the intermediate progenitor hypothesis, which proposes that expansion of BPs leads to increased cortical surface and formation of cortical folds (Kriegstein *et al*, 2006; Molnar *et al*, 2006), except that the larger cortex of 4D mice remained unfolded. Nevertheless, cortical surface in 4D mice was less than 10%

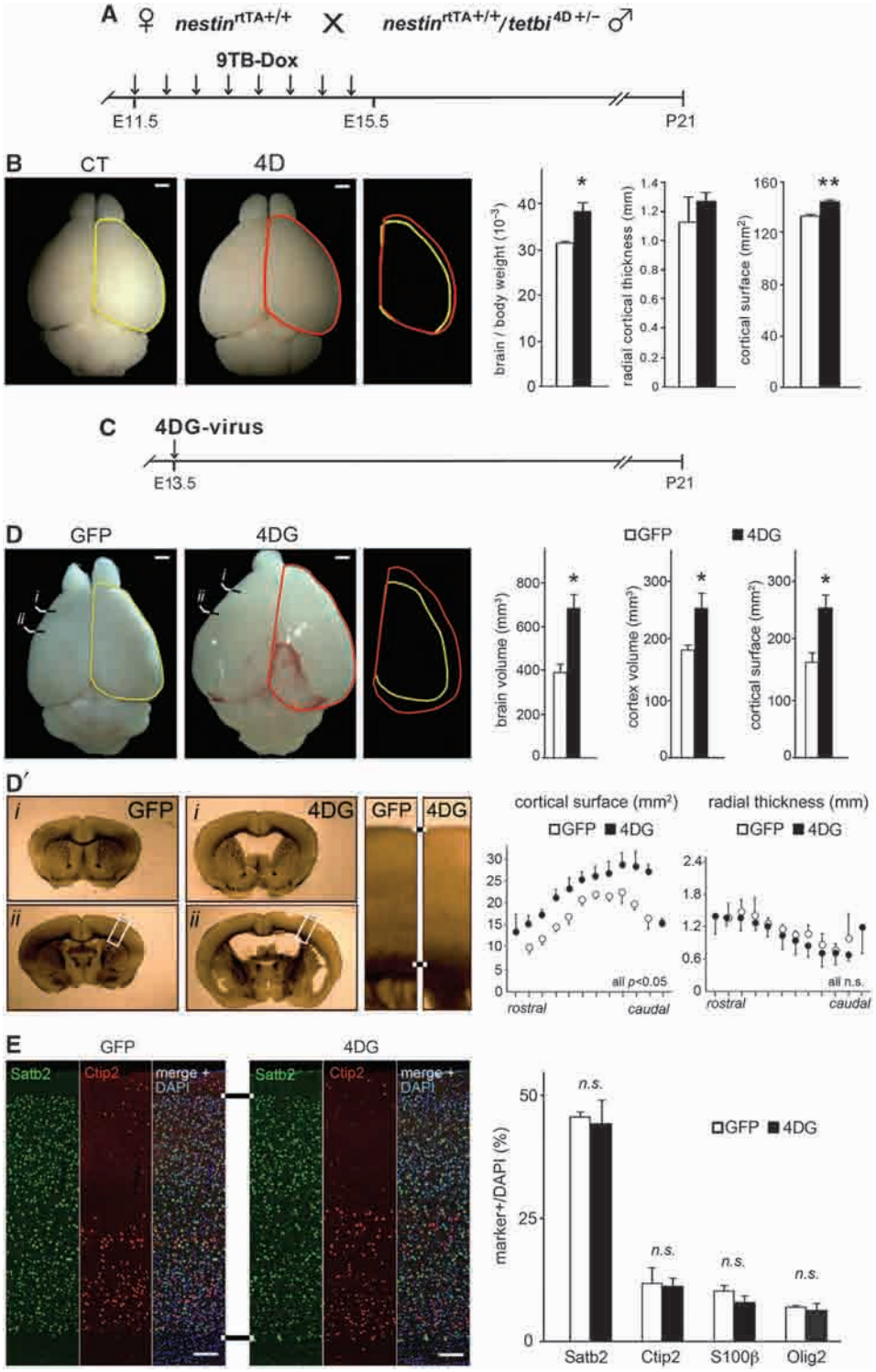

Figure 4 4D expression expands cortical surface area without folding at P21. (**A**) Experimental approach used to study the effect of 4D overexpression after continous administration of 9TB-Dox from E11.5 to E15.5 followed by sacrifice at P21. (**B**) Same magnification whole mount pictures (left) and encephalization measurements (brain relative to body weight, cortical thickness and surface; right) of P21 CT (white) or 4D (black) brains treated with 9TB-dox form E11.5 to E15.5. Yellow and red lines are overlapped to appreciate size differences. (**C**) Experimental approach used to study the effect of 4D overexpression after one single injection of 4DG viruses at E13.5 followed by sacrifice at P21. (**D–D′**) Phase contrast whole mount pictures (left) and quantifications (right) of P21 brains (**D**), and representative coronal sections (**D′**), infected with GFP or 4DG viruses at E13.5. (**E**) Fluorescence pictures and quantifications of cells positive for neuronal and glial markers, as indicated in each panel, in P21 brains treated as in (**C**). Graphs indicate topological measurements of the whole brain (**D**), individual sections (**D′**) or proportion of cell types in the CP (**E**). Scale bars, 100 μm. Data are mean ± s.e.m.; $*P<0.05$; n.s. = not significant; $n=3$ pairs of embryos. See also Supplementary Figure S3.

larger than in controls, and this might be insufficient to drive cortical folding. To test whether dramatically increasing the abundance of BPs might suffice to cause gyrification, we sought to maximise BP expansion by overexpressing 4D at higher levels and for a longer period of time. To this aim, we injected high-titre lentiviruses encoding 4D and GFP (4DG) under a strong constitutive promoter (Artegiani *et al*, 2011) into the telencephalic ventricles of E13.5 embryos and analysed them after prolonged 4D overexpression at P21 (Figure 4C). In contrast to mice infected with GFP alone, 4DG-mice were megalencephalic, with a massive increase in brain volume and enlarged parietal bones (Figure 4D and data not shown). Although 4DG mice were also hydrocephalic, a significant part of their brain enlargement was due to a 42% increase in cortical tissue compared to GFP controls (Figures 4D and D′ and Supplementary Figure S3A). Cortical enlargement was exclusively due to a 57% larger cortical surface, whereas thickness was indistinguishable from controls (Figure 4D′ and Supplementary Figure S3A). Moreover, cells positive for neuronal (Satb2 and Ctip2) or glial (Olig2 and S100β) markers were found in the same density, locations and proportions in GFP and 4DG-infected cortices (Figure 4E, and Supplementary Figures S3B and C), indicating augmented neurogenesis and gliogenesis without disrupting cell specification, lamination or cortical cytoarchitecture. Importantly, despite the massive expansion in cortical surface of 4DG mice, we never detected signs of cortical folding (Figures 4D and D′ and Supplementary Figure S3A). This demonstrated that although dramatic expansion of BPs leads to increased cortical surface, this alone is not sufficient to cause gyrencephaly in naturally lissencephalic species like mouse.

4D overexpression triggers the expansion of ISVZ and OSVZ progenitors

Recent studies have shown that gyrencephalic mammals, including ferret, macaque and human, share a very complex mixture of BP cell types distributed across two germinal layers: the inner and outer SVZ (ISVZ and OSVZ) (Bayatti *et al*, 2008; Fietz *et al*, 2010; Hansen *et al*, 2010; Martinez-Cerdeno *et al*, 2012; Reillo and Borrell, 2012). In these species, a new type of cortical progenitor was recently identified as bRG. These cells also occupy basal positions but share features with the apical RGCs. bRGs are scarce in mice (Shitamukai *et al*, 2011; Wang *et al*, 2011) but very abundant in gyrencephalic species and have been proposed to increase the number of radial units at the pial surface, which might be critical for the development of gyrencephaly (Fietz and Huttner, 2011; Lui *et al*, 2011; Borrell and Reillo, 2012). To elucidate this issue we next tested whether amplification of ISVZ/OSVZ progenitors in the naturally gyrencephalic ferret could also be achieved by overexpression of 4D.

To investigate the acute effects of 4D overexpression we electroporated P1 ferrets with DNA plasmids encoding 4D (as previously performed in mouse; Lange *et al*, 2009), and 5 days later at P6, we analysed the abundance of mitotic cells. In both the VZ and SVZ, the density of PH3+ cells in 4D-electroporated ferrets was two-fold increased compared to ferrets electroporated with control vectors (Figure 5A). This demonstrated that, similar to mouse, 4D overexpression also results in the expansion of cortical progenitors in naturally gyrencephalic species.

We next studied the long term consequences of 4D overexpression on proliferation of ferret neural progenitors. To this aim we performed stereotaxic injections of 4D-encoding retroviruses into the OSVZ of the prospective splenial gyrus of P1 ferrets, and analysed their brains at P30. We chose retroviral vector injection instead of DNA electroporation to avoid the dilution of the episomal electroporated plasmids, and to target primarily progenitors within the OSVZ. Consistent with the expected effect on progenitor cell amplification, we found that at P30 the density of transduced cells was 3.5-fold higher in animals injected with 4D than with control GFP viruses (Figure 5B, bottom right). In addition, we found that in the cortical region containing 4D+ cells a high abundance of mitotic cells were still present even at this late stage of cortical maturation (Figure 5B). Given that cortical progenitor proliferation should have been over long before P30, this result prompted us to investigate if 4D overexpression might lead to a general delay in neurogenesis and cortical maturation. To this aim we examined in detail the cellular phenotype of 4D or CT-expressing cells, and found that in 4D ferrets the proportion of GFP+ neurons relative to glia was dramatically increased, from 11 to 50% (Figure 4C). Importantly, while the majority of neurons in CT animals exhibited large-cell somas with distinct dendritic and axonal arbours, indicative of differentiated neurons (Figure 5C, blue arrowheads), in 4D animals the vast majority of neurons had a typical migratory appearance, suggestive of developmental delay (Figure 5C, red arrowheads). Taken together, these results are consistent with 4D inducing an increased but delayed neurogenesis.

4D overexpression triggers the formation of new cortical folds in naturally gyrencephalic brains

After confirming that 4D overexpression induced OSVZ progenitor proliferation we next studied the long term consequences of this progenitor expansion on the mature cerebral cortex. In particular we investigated whether this manipulation of OSVZ progenitors might promote additional cortical folding or rather, similar to mouse, it would only expand cortical surface area without additional gyrification. High-titre 4D-encoding retroviruses were injected into the OSVZ as above, and topology of the P30 visual cortex was assessed by stereological measurement of cortical surface. Whereas GFP virus injection produced no significant change compared to the uninjected hemisphere, 4D increased the perimeter of the splenial gyrus by 20%. Remarkably, this increase in cortical surface area came together with the formation of inward folds of the cortical mantle, which increased the local gyrification index by 33% (Figures 6A, B and D). Importantly, these *de novo* cortical folds had a normal laminar organisation, as assessed by Cux1, Ctip2 and DAPI stains (Figures 6B and C). Thus, in contrast to mouse, expansion of OSVZ progenitors in the naturally gyrencephalic ferret was sufficient to trigger the *de novo* formation of cortical folds.

Discussion

A number of genetic systems have been described in recent years that allow the manipulation of stem cell activity *in vivo*. In particular for Cdks and cyclins, it has been proposed that these cell cycle regulators can promote the expansion of stem cells in a number of contexts including embryonic pluripotent

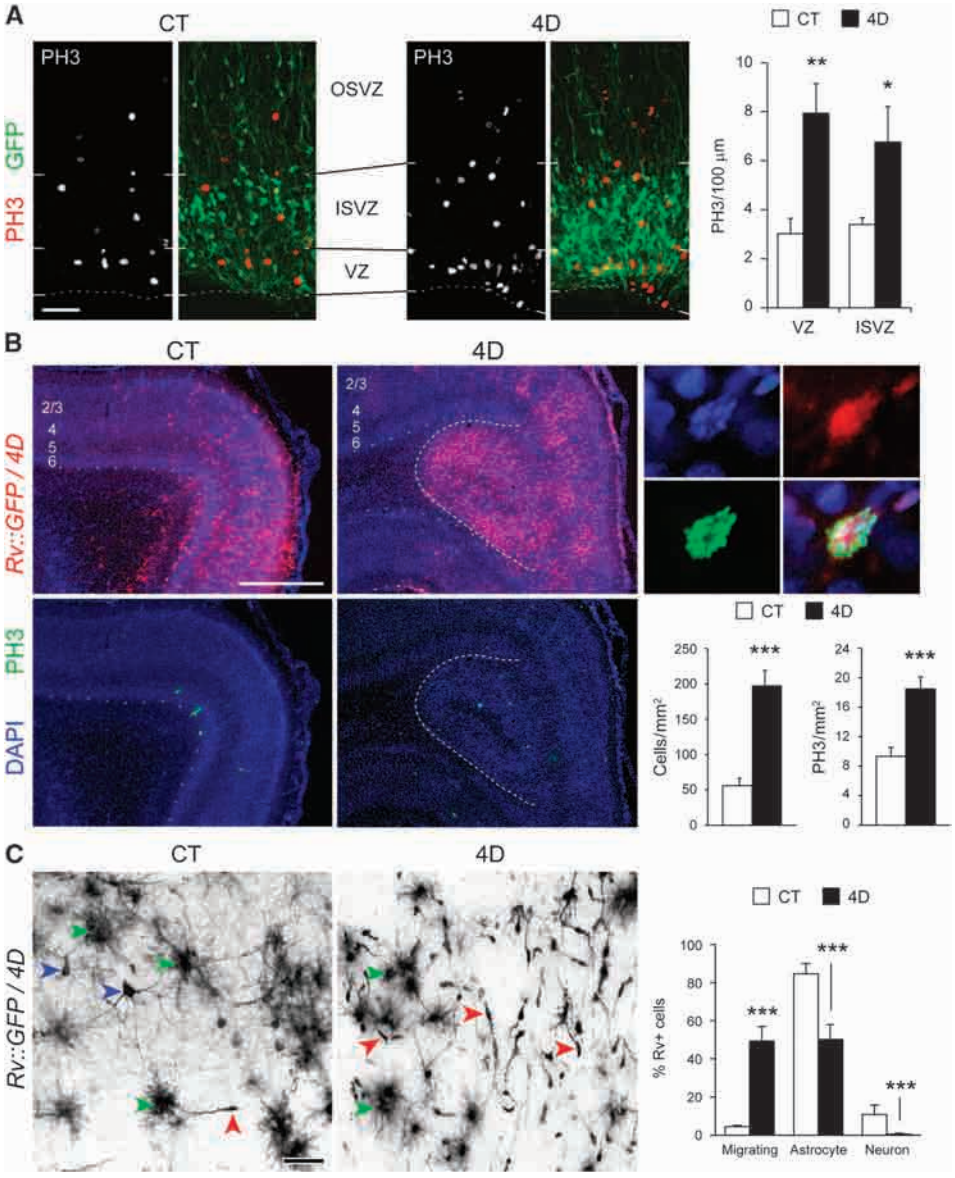

Figure 5 4D overexpression triggers the expansion of ferret neural progenitors. (**A**) Fluorescence pictures and quantification of cells labelled for PH3 in P6 ferrets electroporated at P1 with GFP (CT) or GFP + 4D-encoding plasmids (4D). Note the increased number of PH3 + cells in 4D. (**B**) Fluorescence pictures of the splenial gyrus of a P30 ferret injected at P1 in the OSVZ with CT- (left) or 4D- (right) retroviruses (red) followed by immunohistochemistry with PH3 (green) and DAPI counterstaining (blue). Numbers indicate cortical layers. Details (top right) show a transduced cell in mitosis. Quantifications (bottom right) shown the increase in proliferation and in the density of transduced cells caused by 4D overexpression. Note the inward cortical fold (dashed line) formed after 4D overexpression as seen in cross-section. (**C**) GFP + cells labelled with black reaction product in the cortical grey matter of P30 ferrets treated as in (**B**) and quantification of cell types based on morphology (right). Note the dramatically higher proportion of newborn migrating neurons in 4D brains relative to CT, together with a reduction in mature astrocytes and neurons (red, green and blue arrowheads, respectively). Scale bars, 50 µm (**A**) or 1 mm (**B**) or 60 µm (**C**). Data are mean ± s.e.m. ***$P<0.001$; $n = 12\,946$ cells, four animals.

stem cells (Singh and Dalton, 2009), hematopoietic stem cells (Orford and Scadden, 2006) as well as neural stem cells during both embryonic development (Calegari and Huttner, 2003; Lange *et al*, 2009) and adulthood (Artegiani *et al*, 2011) (reviewed by Salomoni and Calegari, 2010; Lange and Calegari, 2010). However, to our knowledge no system has previously been shown to be at the same time sufficiently potent and specific to allow an increase in organ size without any obvious impairment in neither organ structure nor function. Based on the effects of 4D on brain size (current work) and their proposed roles on other stem cell types (mentioned above), the combination of the mouse line for rtTA-dependent expression of 4D here described with relevant rtTA-transactivator lines will make it an invaluable tool for the expansion of stem cells in a time- and cell type-specific manner. Thus, our system provides a powerful, practical and extremely versatile approach to assess stem cell contribution to tissue formation and homoeostasis in virtually any tissue during both embryonic development and adulthood. Indeed, in the present study we have combined our new mouse line

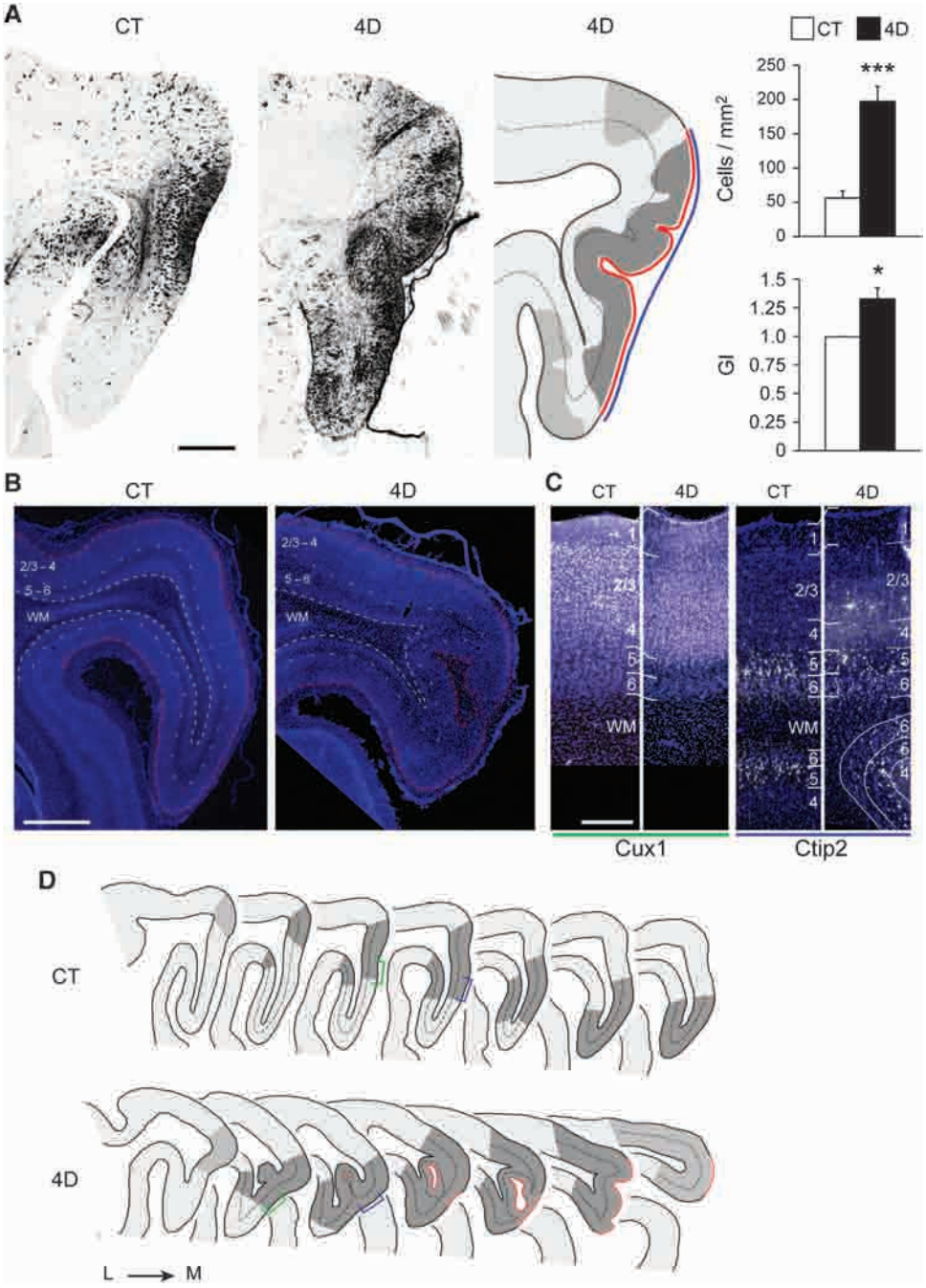

Figure 6 4D overexpression in ferret elicits *de novo* cortical folding. (**A**, **D**) Pictures, schematic reconstructions and quantifications of sagittal sections of the splenial gyrus of P30 ferrets injected at P1 in the OSVZ with retro-GFP (CT) or retro-4D (4D). Transduced cells are labelled with black reaction product. Plots represent density of transduced cells and local GI within the targeted region. Dark and light grey shading indicates areas with high and low density of transduced cells, respectively; dashed lines indicate trajectory of layer 4, red line indicates cortical surface affected by 4D expression and blue line indicates outer contour of the cortex used to calculate cortical perimeter and local GI. Color-coded brackets in D indicate regions shown in C. L, lateral; M, medial. (**B**, **C**) Fluorescence pictures from brain sections of cortical regions with high density of transduced cells in CT or 4D injected ferrets stained for DAPI (**B**) or for Cux1 and Ctip2 (**C**, white) illustrating the normal laminar arrangement of the expanded cerebral cortex of 4D animals. In 4D stained for Ctip2, cortical layers are seen to wrap around at the level of the tissue engulfment, as in **D**, deep below their standard superficial position. Scale bars, 1 mm (**A** and **B**) or 200 μm (**C**). Data are mean ± s.e.m.; $n = 3$ sections/animal, 2–3 animals/group; $^{*}P < 0.05$, $^{**}P < 0.01$, $^{***}P < 0.0001$.

with a *nestin*^{rtTA} line to investigate the involvement of neural progenitor subtypes in the establishment of brain size and morphology during embryonic development.

In the last decades, the characterisation of neural stem and progenitor cell types in the mammalian cortex has led to a number of hypotheses that subsequently attempted to explain the cellular mechanisms responsible for the increase in brain size and folding during mammalian evolution. Clearly, a major interest for this area of research is fuelled by the concept that increased brain size and folding underlie higher cognitive and intellectual performance, thus aiming towards the long-dated quest for understanding what makes us

human. Several experimental studies have attempted to address this issue, and some were successful in generating mice with an enlarged cortex (Chenn and Walsh, 2002; Cappello *et al*, 2006; Siegenthaler *et al*, 2009). However, the experimental manipulations in those studies also induced major defects in neurogenesis, neuronal survival, lamination and/or specification, and thus fell short from dissecting the cellular mechanisms that specifically control cortical thickness, surface area or folding.

Here we have followed two distinct and independent approaches to show that in both lissencephalic and gyrencephalic species the specific expansion of BPs increases the surface area of the cerebral cortex while preserving normal lamination, thickness and neuronal specification. In this context, this is the first demonstration that the relative abundance of BPs exerts a profound influence on the surface area size of a normally-laminated cerebral cortex, both in lissencephalic and gyrencephalic species. In addition, we have shown that augmented proliferation of progenitors in the OSVZ of the naturally gyrencephalic ferret led to the formation of extra cortical folds. In contrast, in the lissencephalic mouse increased proliferation in the SVZ *per se* was not sufficient to cause gyrification, even in the extreme case of massively megalencephalic brains, which nevertheless remained lissencephalic. Given that the major distinction between the SVZ in mouse and the OSVZ in ferret is the dramatically different proportions of bRGs relative to BPs (Fietz *et al*, 2010; Hansen *et al*, 2010; Lui *et al*, 2011; Reillo *et al*, 2011; Borrell and Reillo, 2012), our current findings strongly support the notion that variations in surface area versus folding across mammalian phylogeny are caused by the differential contribution to cortical development of these two types of basal progenitor cells (Borrell and Reillo, 2012; Kelava *et al*, 2012).

Our findings are consistent with current models in which bRG is proposed to play primary roles in cortical surface area expansion and folding (Lui *et al*, 2011; Borrell and Reillo, 2012; Kelava *et al*, 2012) and complement a recent study inducing gyrification in the mouse cerebral cortex by manipulating a novel nuclear protein affecting BPs and bRG amplification (Stahl *et al*, in press). In contrast, our experimental data challenge previous models. In particular, the radial unit hypothesis (Rakic, 1995) proposed that cortical surface area is determined by the number of VZ radial units, but in our 4D mice cortical surface was massively increased without expansion of RGCs in the VZ. The intermediate progenitor hypothesis (Kriegstein *et al*, 2006; Molnar *et al*, 2006) proposed that the relative abundance of BPs relative to RGCs determines both cortical size and folding, but even a massive expansion of BPs was not sufficient to cause gyrencephaly in 4D mice. Of note, the similar cortical thickness and lamination, and overtly delayed neurogenesis upon progenitor expansion in mouse, revises the long-held assumption that neuronal subtypes may be established by intrinsic developmental clocks counting the number of consecutive progenitors divisions (Caviness *et al*, 1995; Durand and Raff, 2000).

Altogether, our study provides the first experimental model in which cortical expansion and folding were increased without disrupting neuronal composition and cytoarchitecture, offering new insights into the evolutionary increase in brain size underlying greater intellectual performance.

Materials and methods

Generation and use of 4D mice

The *tetbi*^{4D} responder construct was obtained by inserting Cdk4-T2A and Cyclin D1-T2A-RFP fragments (Artegiani *et al*, 2011) in the pBI-L vector (Clontech) coding for luciferase under a bidirectional *tetbi*. Responder lines were generated by pronuclear injection of C57BL/6 mouse zygotes and lines screened individually for doxycycline-dependent induction of 4D (Supplementary data, Experimental procedures, and Figure S1). The best *tetbi*^{4D} responder, relative to leakiness, was then crossed to transactivator *nestin*^{rtTA} mice (Mitsuhashi *et al*, 2001) (Jackson Laboratory) until obtaining *nestin*$^{rtTA+/+}$/*tetbi*$^{4D+/-}$ mice that were backcrossed to *nestin*$^{rtTA+/+}$ to obtain a similar proportion of 4D$^{+/-}$ as well as 4D$^{-/-}$ mice that were used as internal negative control. 4D induction was achieved by intraperitoneal injection of 1 mg of 9TB-dox (Partek Pharmaceuticals, Inc.) in 100 µl distilled water twice a day while 1.2 mg BrdU (Sigma) was used for proliferation or birth-dating analyses.

Surgery and viral injection

HIV lentiviral suspensions were prepared as previously described (Artegiani *et al*, 2011) and ca. 1 µl injected intraventricularly in E13.5 mouse embryos. In ferret, anaesthetised P1 kits were either injected with plasmids and electroporated in the VZ of the occipital cerebral cortex or, alternatively, injected with 4 µl of MLV retroviral suspension into the OSVZ by means of a stereotaxic frame as previously described (Borrell, 2010; Reillo *et al*, 2011) (see also Supplementary Experimental Procedures).

Immunohistochemistry and stereology

Embryonic mouse brains were fixed overnight in 4% paraformaldehyde in 120 mM phosphate buffer pH 7.4 (PFA), while postnatal mice and ferrets were anaesthetised with a mixture of Ketamine (Pfizer) and Xylazine (0.1 mg and 0.5 ml/g body weight, respectively) (Bayer), transcardially perfused with PBS followed by PFA and brains postfixed overnight at 4 °C. Whole mount brains were analysed for endogenous fluorescence using a stereomicroscope equipped with epifluorescence and embedded in 4% low-melting agarose (Invitrogen) to obtain vibratome sections (mouse) or cryoprotected in 30% sucrose and freeze-cut (ferret). Immunohistochemistry was performed on 50 µm thick sections as described in Supplementary Experimental Procedures and Supplementary Table S1. For stereology in mouse, coronal vibratome sections from the most anterior part of the telencephalon until its end were collected. Sections of different thickness were performed to account for the different size of the brain with 50 µm chosen for analyses at E15.5 and E18.5; 100 µm at P21; and 150 µm for GFP and 4DG viral infected megalencephalic P21 brains. One every fourth consecutive section was photographed using an automated microscope (ApoTome; Carl Zeiss), pictures digitally assembled using Axiovision software (Carl Zeiss) and composites analysed using Photoshop CS4 (Adobe) or ImageJ 1.33 to calculate the perimeter of the ventricular and cortical surfaces and thickness of the cortical layers that were used to calculate surface areas and volumes by multiplying the sum of each by the distance between consecutive sections. Stereology in ferrets was performed using Neurolucida software on sections containing GFP+, targeted cells using the controlateral, unmanipulated hemisphere as internal negative control. The perimeter of the splenial gyrus, the portion of this gyrus containing transduced cells and the equivalent portion of the contralateral hemisphere were measured following the border between L2/3 and L1 or the outer border of the cortex. Gyrification index was measured in the cortical region containing a high density of transduced cells by dividing the outer border by the L2/3-L1 perimeter.

Statistical analyses

Mouse cells were counted in a column of 100 µm of lateral cortical wall within field 40 comparing sections at identical antero-posterior levels of the brain, as identified by stereological analyses. Similarly, ferret cells were counted in a column orthogonal to the ventricular surface within the GFP+ targeted area of the prospective splenial gyrus and represented as number of cells per cortical column of 100 µm width at the level of the VZ. In all quantifications, boundaries between VZ, SVZ, IZ, and CP were identified by immunor-

eactivity for the RGC marker Pax6, the BP marker Tbr2, and/or by cytoarchitecture using DAPI. Mean and standard error of the mean were calculated on two to eight brains obtained from two to five litters with *P*-values being calculated by Student's *t*-test.

Supplementary data

Supplementary data are available at *The EMBO Journal* Online (http://www.embojournal.org).

Acknowledgements

We thank Dr M Hasan for advice, K Anastassiadis, R Neumann for mouse transgenesis and the MPI-CBG and UMH for animal husbandry. This work was supported by the Ministerio de Ciencia e Innovación (IR, AP2008-01264; VB, SAF2009-07367 and CONSOLIDER CSD2007-00023), European Research Council (VB, 309633), DFG Collaborative Research Center SFB655 (subproject A20), Center for Regenerative Therapies and Medical Faculty of the TU Dresden (FC).

Author contributions: MNK, IR, BA, MAMM, VB and FC designed, performed and analysed the experiments; MN provided reagents; VB and FC conceived the project and prepared the manuscript.

Conflict of interest

The authors declare that they have no conflict of interest.

References

Artegiani B, Lindemann D, Calegari F (2011) Overexpression of cdk4 and cyclinD1 triggers greater expansion of neural stem cells in the adult mouse brain. *J Exp Med* **208:** 937–948

Bayatti N, Moss JA, Sun L, Ambrose P, Ward JF, Lindsay S, Clowry GJ (2008) A molecular neuroanatomical study of the developing human neocortex from 8 to 17 postconceptional weeks revealing the early differentiation of the subplate and subventricular zone. *Cereb Cortex* **18:** 1536–1548

Borrell V (2010) *In vivo* gene delivery to the postnatal ferret cerebral cortex by DNA electroporation. *J Neurosci Meth* **186:** 186–195

Borrell V, Reillo I (2012) Emerging roles of neural stem cells in cerebral cortex development and evolution. *Dev Neurobiol* **72:** 955–971

Calegari F, Huttner WB (2003) An inhibition of cyclin-dependent kinases that lengthens, but does not arrest, neuroepithelial cell cycle induces premature neurogenesis. *J Cell Sci* **116:** 4947–4955

Cappello S, Attardo A, Wu X, Iwasato T, Itohara S, Wilsch-Brauninger M, Eilken HM, Rieger MA, Schroeder TT, Huttner WB, Brakebusch C, Götz M (2006) The Rho-GTPase cdc42 regulates neural progenitor fate at the apical surface. *Nat Neurosci* **9:** 1099–1107

Caviness Jr. VS, Takahashi T, Nowakowski RS (1995) Numbers, time and neocortical neuronogenesis: a general developmental and evolutionary model. *Trends Neurosci* **18:** 379–383

Chenn A, Walsh CA (2002) Regulation of cerebral cortical size by control of cell cycle exit in neural precursors. *Science* **297:** 365–369

de Felipe P, Luke GA, Hughes LE, Gani D, Halpin C, Ryan MD (2006) E unum pluribus: multiple proteins from a self-processing polyprotein. *Trends Biotechnol* **24:** 68–75

Durand B, Raff M (2000) A cell-intrinsic timer that operates during oligodendrocyte development. *Bioessays* **22:** 64–71

Englund C, Fink A, Lau C, Pham D, Daza RA, Bulfone A, Kowalczyk T, Hevner RF (2005) Pax6, Tbr2, and Tbr1 are expressed sequentially by radial glia, intermediate progenitor cells, and postmitotic neurons in developing neocortex. *J Neurosci* **25:** 247–251

Fietz SA, Huttner WB (2011) Cortical progenitor expansion, self-renewal and neurogenesis-a polarized perspective. *Curr Opin Neurobiol* **21:** 23–35

Fietz SA, Kelava I, Vogt J, Wilsch-Brauninger M, Stenzel D, Fish JL, Corbeil D, Riehn A, Distler W, Nitsch R, Huttner WB (2010) OSVZ progenitors of human and ferret neocortex are epithelial-like and expand by integrin signaling. *Nat Neurosci* **13:** 690–699

Gotz M, Huttner WB (2005) The cell biology of neurogenesis. *Nat Rev Mol Cell Biol* **6:** 777–788

Hansen DV, Lui JH, Parker PR, Kriegstein AR (2010) Neurogenic radial glia in the outer subventricular zone of human neocortex. *Nature* **464:** 554–561

Haubensak W, Attardo A, Denk W, Huttner WB (2004) Neurons arise in the basal neuroepithelium of the early mammalian telencephalon: A major site of neurogenesis. *Proc Natl Acad Sci USA* **101:** 3196–3201

Kelava I, Reillo I, Murayama AY, Kalinka AT, Stenzel D, Tomancak P, Matsuzaki F, Lebrand C, Sasaki E, Schwamborn JC, Okano H, Huttner WB, Borrell V (2012) Abundant occurrence of basal radial glia in the subventricular zone of embryonic neocortex of a lissencephalic primate, the common marmoset Callithrix jacchus. *Cereb Cortex* **22:** 469–481

Kriegstein A, Noctor S, Martinez-Cerdeno V (2006) Patterns of neural stem and progenitor cell division may underlie evolutionary cortical expansion. *Nat Rev Neurosci* **7:** 883–890

Lange C, Calegari F (2010) Cdks and cyclins link G(1) length and differentiation of embryonic, neural and hematopoietic stem cells. *Cell Cycle* **9:** 1893–1900

Lange C, Huttner WB, Calegari F (2009) Cdk4/cyclinD1 overexpression in neural stem cells shortens G1, delays neurogenesis, and promotes the generation and expansion of basal progenitors. *Cell Stem Cell* **5:** 320–331

Lui JH, Hansen DV, Kriegstein AR (2011) Development and evolution of the human neocortex. *Cell* **146:** 18–36

Malatesta P, Hartfuss E, Gotz M (2000) Isolation of radial glial cells by fluorescent-activated cell sorting reveals a neuronal lineage. *Development* **127:** 5253–5263

Martinez-Cerdeno V, Cunningham CL, Camacho J, Antczak JL, Prakash AN, Cziep ME, Walker AI, Noctor SC (2012) Comparative analysis of the subventricular zone in rat, ferret and macaque: evidence for an outer subventricular zone in rodents. *PLoS One* **7:** e30178

Mitsuhashi T, Aoki Y, Eksioglu YZ, Takahashi T, Bhide PG, Reeves SA, Caviness Jr. VS (2001) Overexpression of p27Kip1 lengthens the G1 phase in a mouse model that targets inducible gene expression to central nervous system progenitor cells. *Proc Natl Acad Sci USA* **98:** 6435–6440

Miyata T, Kawaguchi A, Okano H, Ogawa M (2001) Asymmetric inheritance of radial glial fibers by cortical neurons. *Neuron* **31:** 727–741

Miyata T, Kawaguchi A, Saito K, Kawano M, Muto T, Ogawa M (2004) Asymmetric production of surface-dividing and non-surface-dividing cortical progenitor cells. *Development* **131:** 3133–3145

Molnar Z, Metin C, Stoykova A, Tarabykin V, Price DJ, Francis F, Meyer G, Dehay C, Kennedy H (2006) Comparative aspects of cerebral cortical development. *Eur J Neurosci* **23:** 921–934

Molyneaux BJ, Arlotta P, Menezes JR, Macklis JD (2007) Neuronal subtype specification in the cerebral cortex. *Nat Rev Neurosci* **8:** 427–437

Noctor SC, Flint AC, Weissman TA, Dammerman RS, Kriegstein AR (2001) Neurons derived from radial glial cells establish radial units in neocortex. *Nature* **409:** 714–720

Noctor SC, Martinez-Cerdeno V, Ivic L, Kriegstein AR (2004) Cortical neurons arise in symmetric and asymmetric division zones and migrate through specific phases. *Nat Neurosci* **7:** 136–144

Orford KW, Scadden DT (2009) Deconstructing stem cell self-renewal: genetic insights into cell-cycle regulation. *Nat Rev Genet* **9:** 115–128

Rakic P (1995) A small step for the cell, a giant leap for mankind: a hypothesis of neocortical expansion during evolution. *Trends Neurosci* **18:** 383–388

Reillo I, Borrell V (2012) Germinal zones in the developing cerebral cortex of ferret: ontogeny, cell cycle kinetics, and diversity of progenitors. *Cereb Cortex* **22:** 2039–2054

Reillo I, de Juan Romero C, Garcia-Cabezas MA, Borrell V (2011) A role for intermediate radial glia in the tangential expansion of the mammalian cerebral cortex. *Cereb Cortex* **21:** 1674–1694

Salomoni P, Calegari F (2010) Cell cycle control of mammalian neural stem cells: putting a speed limit on G1. *Trends Cell Biol* **5:** 332–342

Shitamukai A, Konno D, Matsuzaki F (2011) Oblique radial glial divisions in the developing mouse neocortex induce self-renewing progenitors outside the germinal zone that resemble primate outer subventricular zone progenitors. *J Neurosci* **31:** 3683–3695

Siegenthaler JA, Ashique AM, Zarbalis K, Patterson KP, Hecht JH, Kane MA, Folias AE, Choe Y, May SR, Kume T, Napoli JL, Peterson AS, Pleasure SJ (2009) Retinoic acid from the meninges regulates cortical neuron generation. *Cell* **139:** 597–609

Singh AM, Dalton S (2009) The cell cycle and Myc intersect with mechanisms that regulate pluripotency and reprogramming. *Cell Stem Cell* **5:** 141–149

Stahl R, Walcher T, De Juan Romero C, Pilz GA, Cappello S, Irmler M, Sanz Anquela JM, Beckers J, Blum R, Borrell V & Götz M (in press) Trnp1 regulates expansion and folding of the mammalian cerebral cortex by control of radial glial fate. doi:10.1016/j.cell.2013.03.027

Wang X, Tsai JW, LaMonica B, Kriegstein AR (2011) A new subtype of progenitor cell in the mouse embryonic neocortex. *Nat Neurosci* **14:** 555–561